The 2017 World Congress on
Advances in Structural Engineering and Mechanics (ASEM17)
28 August - 1 September, 2017, Ilsan(Seoul), Korea

Investigation of Hydrogen Embrittlement of High Strength Pipeline Steels under Typical Service Environment

Yichen Fang[1], Minxu Lu[1], Yunying Xing[2], Hongjie Shen[1] and Lei Zhang[1]

[1] *Institute of Advanced Materials and Technology, University of Science and Technology Beijing, No.30 Xueyuan Road, Haidian District Beijing, 100083 China*
[2] *Safetech Research Institute Room 1702, Haitai Mansion, 229 North 4th Ring Road, Haidian District, Beijing, 100083 China*

ABSTRACT

With the wider application of pipeline steels higher than API X70 grade, the hydrogen embrittlement risk induced by service conditions has been recognized. Since the increased strengthening of pipeline steel might significantly increase the hydrogen cracking sensitivity, a greater understanding on the different criteria of service parameters compared with those of traditional pipeline steels are required. This paper focuses on the hydrogen embrittlement behaviors of API X70 and API X80 high strength pipeline steel in two typical service environments, under cathodic protection in soil simulation conditions and within simulated coal gas environment. The uptake and diffusion of hydrogen in the steels under different condition were analyzed by hydrogen permeation test and hydrogen content measurement. Slow strain rate testing (SSRT) under cathodic conditions as well as mechanical performance degradation testing after long term immersion were used to determine the hydrogen embrittlement (HE) susceptibilities of the two kinds of steel. The results showed the changes of hydrogen diffusion rate, hydrogen accumulation limit and hydrogen embrittlement with the increased steel strength under different cathodic protection conditions or different hydrogen partial pressure.
Key words: high strength pipeline steel; hydrogen embrittlement; cathodic protection; hydrogen permeation; hydrogen content measurement; slow strain rate test

INTRODUCTION

With growing need in energy supply, petroleum industry has paid extensive attention to increase the transport capacity and the safety of pipeline. There has been a noteworthy trend toward increasing the relevant mechanical properties of pipeline steels, particularly as the application of high-strength steel pipeline is cost effective, given the increased pressure of the transmitted oil or gas and the decreased wall thickness of the pipeline [1-4]. However, it is well known that the hydrogen embrittlement (HE) susceptibility of high-strength steel increases with increasing the strength level, cathodic

protection at too negative potentials also can enhance the risks of hydrogen embrittlement [5-8].

In addition to the strength grade of steel, the HE sensitivity of high-strength pipeline steel is also closely related to microstructure, service environment, and current density. As the grade ascends from traditional X60, X70 to X80, X90 and the newest X100, X120, the metallographic structure of pipeline steel change from polygonal ferrite-pearlite to acicular ferrite and bainite [9]. And the susceptibility to hydrogen embrittlement increases in the order of polygonal ferrite, acicular ferrite, bainite [10]. By cathodic protection, corrosion can be effectively controlled. However, cathodic charging is one of the reasons that lead to the hydrogen embrittlement of high strength steel. On the one hand, the amount of absorbed hydrogen in steels is affected by the the pH of the service environment [11-13]. On the other hand, it is also greatly affected by the cathodic protection parameters, such as current density, overpotential and charging time[7-16]. The studies of Yan and Weng indicated that the hydrogen in steels increased as current density (*i*) rose [14]. Devanathan and Stachurski believed that the surface coverage with atomic hydrogen was a constant at higher overpotential, as indicated by the fixed hydrogen permeation into the steel [15]. After charging hydrogen for a long sufficient time, the amount of absorbed hydrogen would be proportional to the applied current density [16,17]. But these researches did not systematically clarify the relationship between hydrogen embrittlement sensitivity and hydrogen diffusion and hydrogen content, and the effect of steel strength, service environment and cathodic protection parameters on it.

This paper investigated the hydrogen embrittlement behaviors of API X70 and X80 high strength pipeline steel under cathodic protection in soil simulation conditions. The uptake and diffusion of hydrogen in the steels under different cathodic protection levels were analyzed by hydrogen permeation test and hydrogen content measurement. Slow strain rate testing (SSRT) under cathodic conditions as well as mechanical performance degradation testing after long term immersion were employed to determine the HE susceptibilities of the three different grades of steels.

EXPERIMENTAL PROCEDURE

Materials and test solutions

Materials used in this study were API X70 and X80 grade pipeline steels. The chemical compositions and mechanical properties are listed in Table 1. The microstructures of the pipeline steels are shown in Fig. 1. The X70 steel's microstructure is constituted by the ferrite and pearlite (Fig. 1-a), while X80 steel revealed the same microstructure and the finer grain (Fig. 1-b). All the specimens were wire-cut EDM tangent to the circle and along the axial direction. Both surfaces were mechanically polished with a series of grit silicon carbide papers (400#, 600#, 800# and 1000#) and cleaned with methanol.

Table 1: Chemical composition (wt%) and mechanical properties of pipeline steels

Grade	C	Mn	Si	P	S	Nb	Mo	Ni	σ_s (MPa)	σ_b (MPa)
X70	0.100	1.66	0.24	0.0090	0.00076	0.058	0.19	0.15	510	620
X80	0.070	1.61	0.21	0.0081	0.00250	0.041	0.13	0.12	550	655

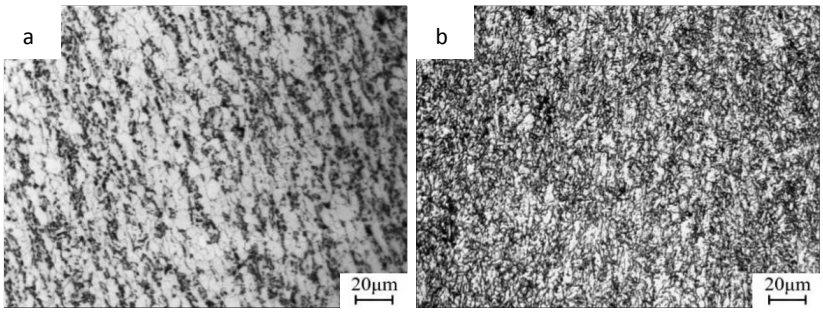

Figure 1: Microstructure of the pipeline steels used in this study (a)X70 (b)X80

The chemical compositions of the soil simulated solutions used in this study were shown in Table 2, which were obtained from the actual service conditions. And the conductivity and pH values of those solutions were measured and shown in Table 2.

Table 2: The soil simulated solutions used in this study (g/L)

content	Ca^{2+}	K^+	Na^+	Mg^{2+}	SO_4^{2-}	Cl^-	HCO_3^-	Conductivity /μS·cm^{-1}	pH value
Solution	0.089	0.015	0.072	＜0.001	0.260	0.026	0.024	504	6.98

Electrochemical hydrogen permeation test

The hydrogen permeation experiments were carried out with a permeation apparatus developed by Devanathan and Stachurski [18] provided with two compartment cells (i.e., hydrogen charging and oxidation cells). Each cell contained a counter electrode and a reference electrode. The cells were separated by the steel specimen which served as the working electrode in both cells. The steel specimen was tightly held between the two cells by rubber gaskets such that the entire system remained leak-tight while avoiding mixing of the solutions on either side of the steel piece. The entry side (i.e., hydrogen charging side) of the specimen at which hydrogen is generated was maintained at a constant cathodic current, whereas an anodic potential was applied on the exit side (i.e., oxidation side) of the specimen. The required current and potential values were applied by a constant-current source and an electrochemical workstation, respectively.

A deaerated 0.1 mol/L NaOH solution was transferred into the oxidation cell and a high-purity nitrogen gas was subsequently bubbled to deaerate the solution. Meanwhile, a constant potential of 300 mV (vs. SCE) was applied on the exit side of the specimen. Once the measured background current decreased to a value below 0.1 μA/cm^2, the test solution was transferred into the hydrogen-charging cell and different cathodic

current densities were applied to the entry sides of the specimens. As a result, hydrogen permeated through the specimen to the oxidation side where it was instantaneously oxidized giving rise to an equivalent current in the exit cell, thereby providing a direct measurement of the output flux of hydrogen. Thus, the electrochemical workstation was used to continuously monitor the anodic current throughout the experiment (i.e., data logging every 2 s).

The hydrogen permeation flux (J_∞) was measured by the steady state permeation current density (I_∞) [19, 20] as shown by the Equation (1):

$$J_\infty = \frac{I_\infty}{nF} \qquad \text{(Eq. 1)}$$

where n is the number of electrons transferred and F is the Faraday constant (F = 96,500 C/mol as reported elsewhere [21, 22]). The sub-surface concentration of hydrogen (c_0) was determined by the following Equation (2) [23-25]:

$$c_0 = \frac{I_\infty L}{nFD_{eff}} \qquad \text{(Eq. 2)}$$

where, as mentioned earlier, D_{eff} in X80 steel at room temperature was determined as 2.00×10^{-6} cm^2/s. The effective hydrogen diffusion coefficients (D_{eff}) can be calculated from the permeation transients using the time-lag method [26] as illustrated in Equation (3) [27]:

$$D = \frac{L^2}{6t_{0.63}} \qquad \text{(Eq. 3)}$$

where L represents the thickness of the specimen, and the time lag $t_{0.63}$ is the elapsed charging time when the ratio of permeation current density to the steady state value (I/I_∞) is equal to 0.63.

Slow strain rate tensile (SSRT) tests

The HIC behavior of high strength steel and the effect of cathodic protection in soil simulated solution were investigated using SSRT methods. The schematic diagram of specimens of SSRT tests is shown in Fig. 2. Prior to testing, the gauge lengths of the specimens were polished to 1200 grit emery paper along the tensile direction, degreased with alcohol, acetone in an ultrasonic cleaner, rinsed with distilled water, and finally dried with hot air. In SSRT tests, a platinum plate and a saturated calomel electrode (SCE) were also immersed in the solution to apply an additional potential before the test and to monitor the changes of corrosion potential of the specimen. However, the platinum counter electrode was removed in the solution during the SSRT test, additional potential was applied to the specimen during the SSRT. The strain rate was controlled at 1×10^{-6} s^{-1}, which was suggested in some references [28, 29].

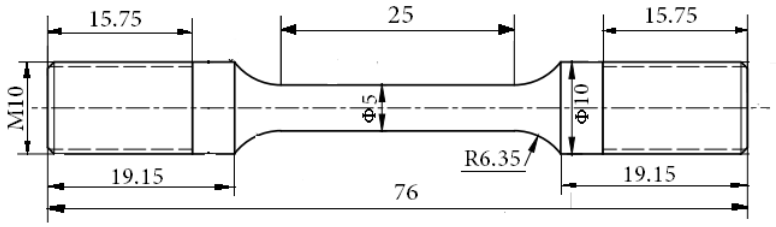

Figure 2: The Schematic diagram of specimens for the samples of SSRT tests (mm)

The reduction of area (Ψ) was usually used to investigate the hydrogen induced ductility loss in test mediums under cathodic protection, and its equation was as follows:

$$\psi = \frac{S_0 - S}{S_0} \times 100\% \quad \text{(Eq. 4)}$$

where S_0 is the cross sectional area of the gauge lengths of the specimens before test, while S is the cross sectional area when the specimens was broken. The susceptibility of hydrogen embrittlement was put forward using the following equation 5:

$$F_H = \frac{\psi_0 - \psi}{\psi_0} \times 100\% \quad \text{(Eq. 5)}$$

where F_H is the hydrogen embrittlement sensitivity coefficient, Ψ_0 is the reduction of area in dry air, and Ψ is the reduction of area in test mediums.

Hydrogen content tests

Hydrogen contained specimens, with a diameter of 10 mm and a height of 10 mm, were immersed in the soil simulated solution. The cathodic charging potential was set to the experimental value and kept for different durations respectively, as shown in Fig.3. Hydrogen content was then immediately detected using Bruke G4 hydrogen determinator.

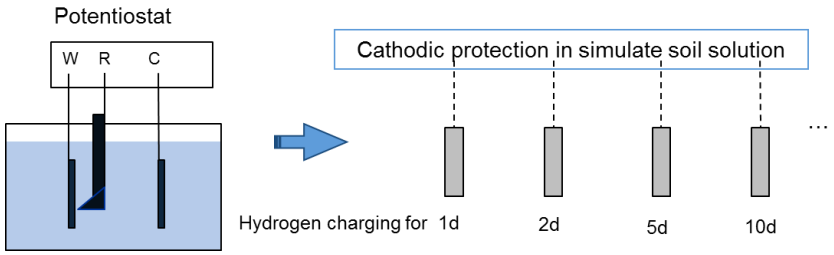

Figure 3: Schematic diagram for hydrogen content tests

RESULTS

The uptake and diffusion of hydrogen in different pipeline steels under cathodic protection

In order to compare the uptake and diffusion behaviors of hydrogen in different pipeline steels under cathodic protection, a series of hydrogen permeation tests were carried out. The cathodic protection potential was set to -1.2V vs. SCE to guarantee enough hydrogen evolution. The results are shown in Fig. 4. The steady state permeation current density (I_∞) of X80 steel was apparently higher than that of X70 steel, this phenomenon revealed the fact that the diffusion of hydrogen atoms into X80 steel was easier.

The correlative hydrogen permeation parameters calculated by the Equations 1- 3 were shown in table 3. The hydrogen permeation flux (J_∞), the sub-surface concentration of hydrogen (c_0), and the effective hydrogen diffusion coefficients (D_{eff}) increased in the order of X70 and X80. This indicated the rate of uptake and accumulation of hydrogen in higher grade steel was quicker, and may lead to higher sensitivity of hydrogen embrittlement.

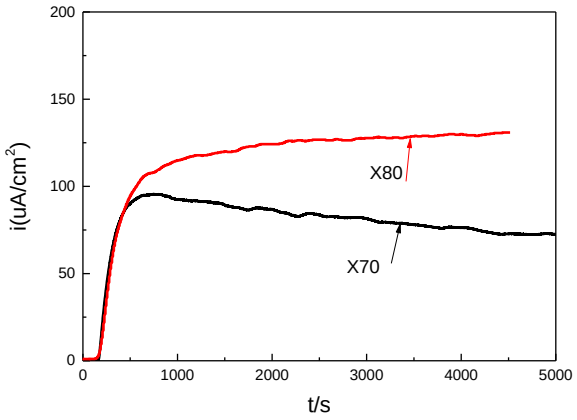

Figure 4: The hydrogen permeation curves of different pipeline steels under -1.2V vs. SCE

Table 3 The correlative hydrogen permeation parameters of different steels under -1.2V vs. SCE

Steel grade	I_∞ (μA/cm^2)	J_∞(×10^{-11}mol H/cm^2/s)	C_0(μmol/cm^3)	D_{eff}(×10^{-6}cm^2/s)
X70	74.40	71.80	1.59	2.01
X80	132.16	127.54	4.45	3.17

Some of the hydrogen in the metal can freely diffuse into the crystal lattice, namely diffusible hydrogen. The contents of diffusible hydrogen of different pipeline steels under -1.2V vs. SCE for different durations were shown in Fig.5. The hydrogen contents in all the three steels show rising trend then decreasing trend with increasing charging time, all the maximum values of the hydrogen contents appeared at about 11days. And the maximum value was larger in the higher grade steel, which indicates higher accumulation ability.

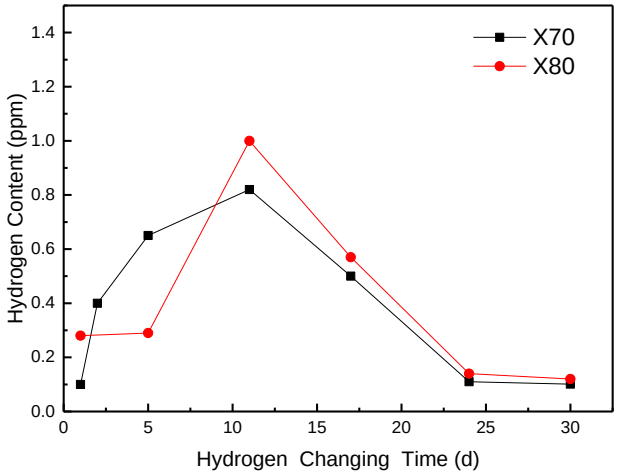

Figure 5: The diffusible hydrogen contents of different steels under -1.2V vs. SCE

The loss of mechanical properties of different pipeline steels under cathodic protection

The susceptibilities of hydrogen embrittlement of the three kinds of steels in the soil simulation solution 2 (in which the calcium ion concentration is in the middle between the rest two) under different cathodic protection potentials were investigated by SSRT. The results are shown in Fig. 8. For the same steel, the more negative the potential, the lower the resulted tensile strength, the strength loss of X80 steel is the more significant than X70.

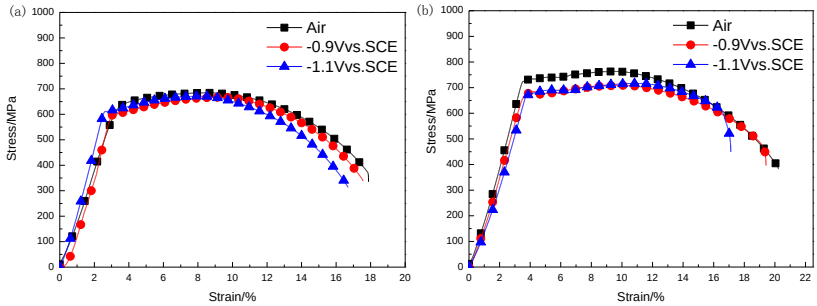

Figure 8: Tension curves of different pipeline steels under different conditions (a) X70 (b) X80

The ductility loss and hydrogen embrittlement susceptibility of the steels were expressed by the reduction of area (Ψ) and hydrogen embrittlement sensitive coefficient (F_H) respectively, which were extracted by Eq. 4 and 5. To compare the hydrogen embrittlement susceptibility of different steels under different conditions, the Ψ and F_H after SSRT is shown in Figures 9 and 10.

Fig. 9 showed that the variation of the reduction of area of X70 steel was the less than X80, which indicates the slight loss of ductility of X70 steel, the ductility loss of X80 steels were more obvious.

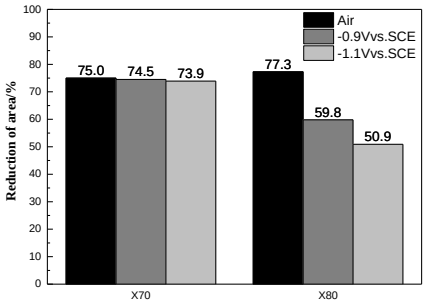

Figure 9: Reduction of area of the different pipeline steels under different conditions

Hydrogen embrittlement sensitive coefficients (F_H) of the three kinds of pipeline steels under different conditions are shown in Fig. 10. The F_H can be used as one of the judging criteria for the possibility of hydrogen embrittlement [30], it is believed that when $F_H < 25\%$, hydrogen embrittlement does not happen; hydrogen embrittlement has potential possibilities when $25\% \leq F_H \leq 35\%$; however, when $F_H > 35\%$, hydrogen embrittlement risk is high. The study shows that with the same cathodic potential, the F_H increases in the order of X70 steel and X80 steel; the more negative the cathodic potential, the higher the F_H. As shown in Fig. 10, the F_H of X80 steel is close to 35% under the cathodic potential of -1.1V vs.SCE, this means that there is the potential possibilities of hydrogen embrittlement, or be greater risk of service.

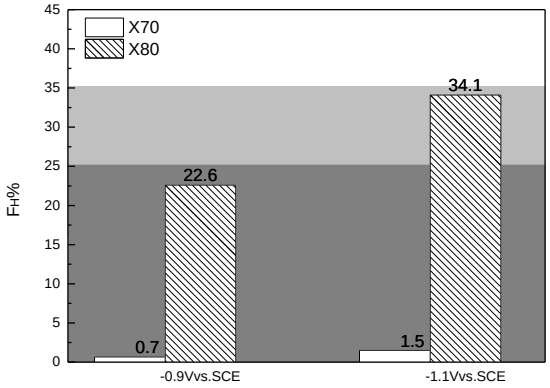

Figure 10: F_H of the two kinds of pipeline steels under different conditions

Baolan Gu [31, 32] considered that the microstructure of the material is one of the important factors that influence the performance of hydrogen induced cracking. The order of resistance of hydrogen induced cracking performance of different microstructures is: ferrite > pearlite > bainite > low-carbon martensite > mixture of martensite and bainite; Gyu [33] discovered that the susceptibility of bainite is much higher than acicular martensite. the microstructure of X80 and X70 is ferrite and pearlite, while the microstructure of X80 is smaller than X70. And take into consideration that the

higher the strength of the steel, the greater the susceptibility of hydrogen embrittlement. Thus considering from strength and structure, the order of hydrogen embrittlement possibilities was X80>X70, slow tensile test results well proved this point.

The research of the behavior of hydrogen and the loss of mechanical properties for pipeline steels in simulated coal gas environment

The susceptibilities of hydrogen embrittlement of simulated coal gas environment were investigated by SSRT. The results are shown in Fig. 11. For the same steel, the strength loss in simulated coal gas environment, the strength loss of X80 steel is the more significant than X70.

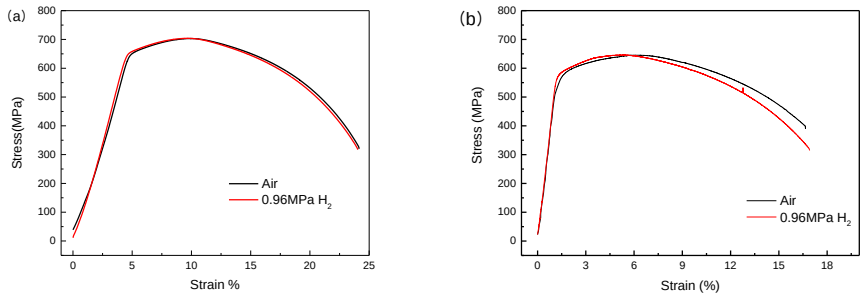

Figure 11: Tension curves of different pipeline steels under simulated coal gas environment(a)X70 (b) X80

The ductility loss and hydrogen embrittlement susceptibility of the steels were expressed by the reduction of area (Ψ) and hydrogen embrittlement sensitive coefficient (F_H) respectively, which were extracted by Eq. 4 and 5. To compare the hydrogen embrittlement susceptibility of different steels under coal gas environment, the Ψ and F_H after SSRT is shown in Figures 12and 13.

Fig. 12 showed that the reduction of area of X70 steel was the less than X80, which indicates the slight loss of ductility of X70 steel, the ductility loss of X80 steels were more obvious.

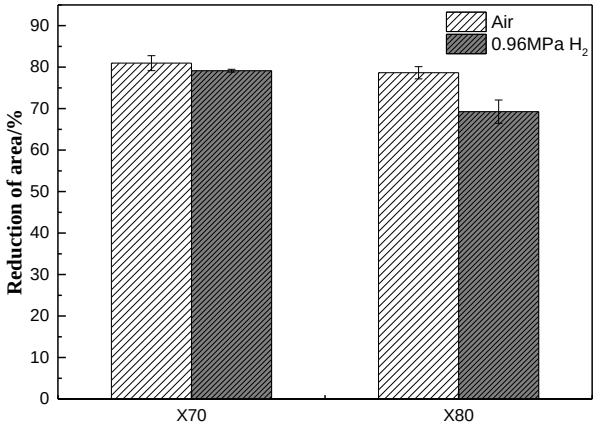

Figure 12: Reduction of area of the different pipeline steels under simulated coal

gas environment

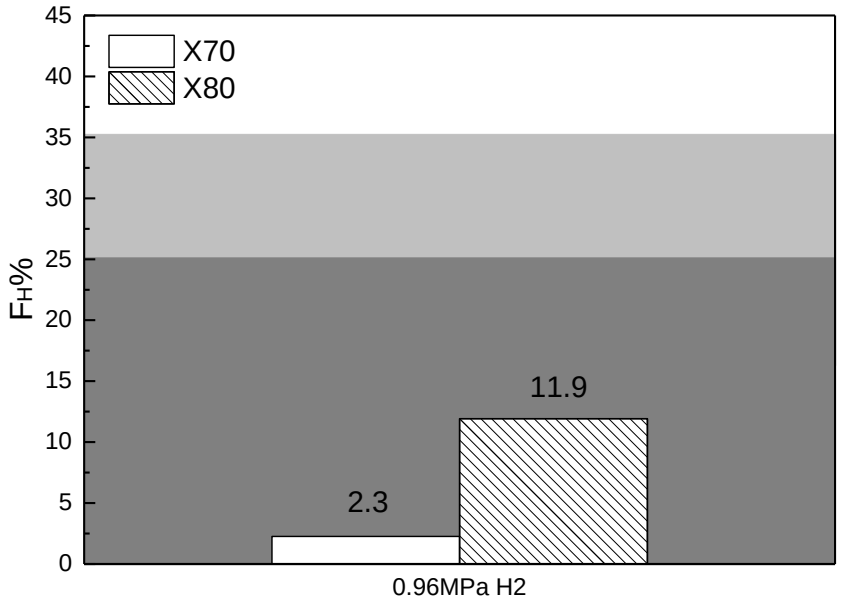

Figure 13: F_H of the two kinds of pipeline steels under simulated coal gas environment

CONCLUSIONS

(1) The uptake and diffusion of hydrogen in the pipeline steels increased in accordance with the sequence of X70, X80 steel, and higher grade of steel indicated higher hydrogen diffusivity.
(2) There existed the maximum value of the hydrogen content in all steels under -1.2 Vvs.SCE for different time. And the maximum value was larger in the higher grade of steel, which represent higher accumulation ability.
(3) For the same grade of steel under cathodic protection, the more negative the applied cathodic potential, the lower the tensile strength, revealing the ductility losses increase with the negative shift of potential.
(4) The ductility loss of X80 steel is the more obvious than X70, and with the negative shift of potential and the increase of steel grade.
(5) The ductility loss of X80 steel is the more obvious than X70 under simulated coal gas environment.

ACKNOWLEDGEMENTS

This work has been supported by National Natural Science Foundation of China (Grant NO. 51271025).

REFERENCES

[1] D. B. Rosado, W. De. Waele, D. Vanderschueren, “Latest developments in mechanical properties and metallurgical features of high strength line pipe steels,” International Conference on Sustainable Construction and Design, (Ghent University, Laboratory Soete, 2013,) p. 41.
[2] H. Hillenbrand, M. Gräf, C. Kalwa. “Development and production of high strength pipeline steels,” Niobium Science & Technology. TMS, (2001): p. 543-569.
[3] I. De S. Bott, L. F.G. De Souza, J. C.G. Teixeira, et al. “High-strength steel development for pipelines: a Brazilian perspective,” Metallurgical and Materials Transactions A 36, 2(2005): p. 443-454.
[4] K. T. Corbett, R. R. Bowen, C. W. Petersen. “High strength steel pipeline economics,” International Journal of Offshore and Polar Engineering 14, 1(2004): p. 75-80.
[5] M. Elboujdaini, W. Revie, “Susceptibility to hydrogen embrittlement under cathodic protection of high-strength pipeline steels,” 14th Middle East Corrosion Conference & Exhibition, Paper no. 61-CP-09, (Manama, Kingdom of Bahrain, February 12-15, 2012).
[6] D. Hardie, E. A. Charles, A. H. Lopez. “Hydrogen embrittlement of high strength pipeline steels,” Corrosion Science 48, 12(2006): p. 4378-4385.
[7] K. Shin-Ichi, R. Maruyama, T. Misawa. “Effect of applied cathodic potential on susceptibility to hydrogen embrittlement in high strength low alloy steel,” ISIJ International 43, 4(2003): p. 475-481.
[8] M. Cabrini, S. Lorenzi, S. Pellegrini, et al. “Environmentally assisted cracking and hydrogen diffusion in traditional and high-strength pipeline steels,” Corrosion Reviews 33, 6(2015): p.529-545.
[9] Y. Ma，H. Li, “Research progress and development direction of pipeline steels and line pipe,” Petroleum Planning & Engineering, 16(2005): p. 1-7.
[10] G. T. Park, S. U. Koh, H. G. Jung, “Effect of microstructure on the hydrogen trapping efficiency and hydrogen induced cracking of linepipe steel,” Corrosion Science 50, 7(2008): p. 1865-1871.
[11] M. Cabrini, S. Lorenzi, P. Marcassoli, et al. “Hydrogen embrittlement behavior of HSLA line pipe steel under cathodic protection,” Corrosion Review 29, 5(2011): p. 261–274.
[12] D. P. Escobar, C. Minambres, L. Duprez, et al. “Internal and surface damage of multiphase steels and pure iron after electrochemical hydrogen charging,” Corrosion Science 53, 10(2011): p. 3166-3176.
[13] C. F. Dong, Z.Y. Liu, X.G. Li, et al, “Effects of hydrogen-charging on the susceptibility of X100 pipeline steel to hydrogen-induced cracking,” International journal of hydrogen energy 34, 24(2009): p. 9879-9884.
[14] M. Yan, Y. Weng, “Study on hydrogen absorption of pipeline steel under cathodic charging,” Corrosion Science 48, 2(2006): p. 432-444.
[15] M. A. V. Devanathan, Z. Stachurski. “The mechanism of hydrogen evolution on iron in acid solutions by determination of permeation rates,” Journal of the electrochemical society 111, 5(1964): p. 619-623.
[16] J Kittel, X Feaugas, J Creus. “Impact of charging conditions and membrane thickness on hydrogen permeation through steel: thick/thin membrane concepts revisited,” CORROSION, paper no. 7848, (Vancouver, BC, Canada, NACE, 2016).

[17] W. Chu. *Hydrogen damage and delayed fracture*, (Beijing, Metallurgy Industry Press, 1988), p. 216.
[18] M. A. V. Devanathan, Z. Stachurski. “The adsorption and diffusion of electrolytic hydrogen in palladium,” Proceedings of the Royal Society A 270, 1340(1962): p. 90-102.
[19] S. H. Wang, W. C. Luu, K. F. Ho, et al. “Hydrogen permeation in a submerged arc weldment of TMCP steel,” Materials Chemistry & Physics 77, 2(2003): p. 447-454.
[20] H B Xue, Y F Cheng. “Hydrogen permeation and electrochemical corrosion behavior of the X80 pipeline steel Weld,” Journal of Materials Engineering & Performance 22, 1(2012): p. 170-175.
[21] Y F Cheng. “Analysis of electrochemical hydrogen permeation through X-65 pipeline steel and its implications on pipeline stress corrosion cracking,” International Journal of Hydrogen Energy 32, 9(2007): p. 1269-1276.
[22] H. B. Xue, Y. F. Cheng. “Characterization of inclusions of X80 pipeline steel and its correlation with hydrogen-induced cracking,” Corrosion Science 53, 4(2011): p.1201-1208.
[23] W. Y. Chu, L. J. Qiao. *Hydrogen embrittlement and stress corrosion*, (Beijing, Science Press, 2013). p.328
[24] C F Dong, K Xiao, et al. “Hydrogen induced cracking of X80 pipeline steel,” Int. J. Miner. Metall. Mater 17, 5(2010): p. 579-586.
[25] R. Nishimura, H. Inoue, K. Okitsu, et al. “Hydrogen permeation behavior in pure nickel implanted with phosphorus, sulphur and their mixture,” Corrosion Science 49, 3(2007): p. 1478-1495.
[26] G. M. Pressouyre, I. M. Bernstein. “A quantitative analysis of hydrogen trapping,” Metallurgical & Materials Transactions A 9, 11(1978): p. 1571-1580.
[27] K. Banerjee, U. K. Chatterjee. “Hydrogen permeation and hydrogen content under cathodic charging in HSLA 80 and HSLA 100 steels,” Scripta Materialia 44, 2(2001): p. 213-216.
[28] P. Liang, C. W. Du, X. G. Li, et al. “Effect of hydrogen on the stress corrosion cracking behavior of X80 pipeline steel in Ku'erle soil simulated solution,” International Journal of Minerals Metallurgy and Materials 16, 4(2009): p. 407-413.
[29] S. X. Mao, L Qiao. “Transgranular cleavage fracture of Fe 3 Al intermetallics induced by moisture and aqueous environments,” Materials Science & Engineering A 258, 2(1998): p. 187-195.
[30] Y. D. Yang, K. D. Lu, W. H. Cao, et al. “Susceptibility of X70 and X80 steels to hydrogen embrittlement in yingtan simulated solution,” Corrosion &Protection 36, 9(2015), p. 810-813.
[31] B. L. Gu, X. D. Xu, L. Zhou. “Study on the effect of pipeline steel microstructure on hydrogen induced cracking,” Physical Testing and Chemical Analysis Part A: Physical Testing 42, 1(2006): p. 8-11.
[32] X.H. Pen. “Study on the hydrogen induced cracking (HIC) behavior of the pipeline steels with different microstructures,” Wuhan university of science and technology, 2013.
[33] T. P. Gyu, U. K. Sung, G. J. Hwan. “Effect of microstructure on the hydrogen trapping efficiency and hydrogen-induced cracking of linepipe steel,” Corrosion Science50, (2008): p.1865-1871